Experimental Study of Precast Segmental Bridge Box Girders with External Unbonded and Internal Bonded Posttensioning under Monotonic Vertical Loading

Aimin Yuan[1]; Yu He[2]; Hang Dai[3]; and Leike Cheng[4]

Abstract: Segmental prestressed-concrete box girders (SPCBGs) with external unbonded and internal bonded posttensioning tendons have been widely used in the construction of bridge structures. These SPCBG bridges have many attractive advantages for ductility and fast construction. However, the behavior of SPCBG bridges is affected by the tendon ratio and the combined load (bending and shear) at the joint surface between the segments. This paper presents an experimental investigation of the structural behavior of SPCBGs with different tendon ratios and combined loads. An experimental study of four different tendon ratios and two types of loads was conducted. The conclusion is that the three-point bending load mode reduced the vertical load and vertical deflection at the onset point of nonlinearity. The openings between the segments and crushing of the concrete compression region are the main reasons for the nonlinear behavior of SPCBGs. Different tendon ratios and different load types not only altered the deformation, increased external tendon stress, and increased the width of joint openings but also altered the failure mechanism. Failure modes of epoxied joints subjected to pure bending or combined shear and bending are presented in detail. For the segmental box girder with external unbonded and internal bonded posttensioning tendons, the stress increment of the external tendons could be up to 30–50% of the effective prestressing stress at the ultimate failure load. Additionally, based on scarce available segmental box-girder test data, several equations on stress increase and shear strength are discussed, and two methods are recommended. **DOI:** 10.1061/(ASCE)BE.1943-5592.0000663. *© 2014 American Society of Civil Engineers.*

Author keywords: Segmental prestressed-concrete beam (SPCB); Hybrid tendon; Combined load; Failure mode; Stress increase.

Introduction

The segmental construction method for prestressed-concrete bridges is fast, safe, and economical and has been widely used in the construction of long-span concrete bridges in China and other countries. However, most applications of the segmental construction method have been restricted to the use of external or internal prestressing (Below et al. 1975; Misic and Warwaruk 1975). The ultimate behavior of externally prestressed segmental bridges is well known to be different from that of internally prestressed bridges. Those differences have already been presented in several papers (Naaman and Alkhairi 1991; Aparicio and Ramos 1996) and are related to the unbonded nature of the external prestressing.

Recently, some segmental bridges, such as the Sutong Yangtze River Bridge and the Nanjing No. 4 Yangtze River Bridge in China, have been designed using external unbonded and internal bonded posttensioning tendons. The analysis of external unbonded and internal bonded posttensioning prestressed segmental box girders presents an additional level of difficulty in comparison with the analysis of conventional internally or externally prestressed box girders because the external unbonded and internal bonded posttensioning prestressing tendon stress at ultimate load cannot be calculated accurately with section analysis. In addition, the ultimate flexural and shear behaviors of a segmental bridge with epoxied joints, multiple shear keys, and external unbonded and internal bonded posttensioning tendons are different because of the presence of internal bonded tendons crossing the joint as well as because of the combination of shear and bending with joint opening.

The unique aspect of the box girders under study lies in the use of external unbonded and internal bonded posttensioning tendons, which are unbonded for external tendons and bonded for internal tendons. Given the presence of internal bonded tendons, the load-carrying capacity of a segmental box girder with external unbonded and internal bonded posttensioning tendons is greater than that of a segmental box girder with only external tendons at the same prestressing tendon ratio. The ductility of the segmental box girder is also improved.

Segmental box girders behave differently under different types of loads, especially in failure. It is critical to understand segmental box-girder performance to determine the design details required to maintain the desired function of the box girder. Some major failures have been attributed to inadequate design parameters under complex load combinations. Therefore, it is crucial to determine the required ratio of the number of internal bonded tendons to external unbounded tendons and to evaluate the ultimate load-carrying capacity of a segmental box girder.

Recent Literature Review

Many investigations of segmental structures have been conducted in the last few decades. An extensive literature review and historical

[1]Associate Professor, Dept. of Civil and Transportation Engineering, Hohai Univ., Nanjing 210098, China (corresponding author). E-mail: yuanam@163.com

[2]Postgraduate Student, Dept. of Civil and Transportation Engineering, Hohai Univ., Nanjing 210098, China. E-mail: 811091228@qq.com

[3]Professor, Dept. of Civil Engineering, Southeast Univ., Nanjing 210096, China. E-mail: hansdai@sina.com

[4]Assistant Engineer, Anhui Transportation Investment Group Co., 180 Camphor Ave., High-Tech Development Zone, Hefei 230088, China. E-mail: erker@126.com

Note. This manuscript was submitted on December 18, 2013; approved on June 16, 2014; published online on July 15, 2014. Discussion period open until December 15, 2014; separate discussions must be submitted for individual papers. This paper is part of the ***Journal of Bridge Engineering***, © ASCE, ISSN 1084-0702/04014075(12)/$25.00.

background on segmental box girders prestressed with external unbonded tendons or internal bonded or unbonded tendons can be found elsewhere (Ramos and Aparicio 1996; Muller 1980; Turmo et al. 2005; Bennett et al. 2002; Rombach 2002). Here, only some test investigations of direct relevance to this study are briefly reviewed.

Only a few investigations have dealt with the influence of combined bending, shear, and torsional loading on the behavior of segmental structures. Algorafi et al. (2010) conducted a series of tests to study the factors involved, including two different external tendon layouts, two types of joints between segments, and different levels of torsional force applied at different load eccentricities. It was concluded that torsion reduces vertical load and vertical deflection. Torsion not only altered the magnitude of the failure load or tendon strain, but it also altered the failure mechanism. Rabbat and Sowlat (1987, 1990) investigated the behavior of two segmental concrete girders incorporating external tendons and made a comparison with that of a similar girder with internal tendons. The results showed that the girders with bonded tendons attained their respective flexural strengths predicted by classical bending theory for monolithic girders. However, the girder with external unbonded tendons exceeded the flexural strength predicted by the provisions of AASHTO specifications (AASHTO 1999). Aparicio et al. (2002) presented the results of a test program on externally prestressed-concrete box girders. Five monolithic and three segmental box girders were tested in bending or in combined bending and shear. The ultimate load capacity of the externally prestressed box girders was found to have a significant influence on tendon length and the shear behavior of open joints. Megally et al. (2009) summarized the seismic performance of precast-concrete segmental bridges. They found that segment joints can undergo large rotations that open gaps in the superstructure without significant loss of strength.

Research Significance

Many problems with segmentally constructed bridges have been found to result from poor construction practices and design errors (Wouters et al. 1999). Internal bonded tendons inevitably present problems, such as anchor corrosion, poor resistance to the repeated application of tension, difficult replacement, and difficulty in predicting the magnitude of the prestressing force. External unbonded tendons also present a problem in that the prestressing force disappears suddenly if the deviator or anchor block breaks down. None of the preceding studies has examined segmental prestressed-concrete box girders (SPCBGs) with both external unbonded and internal bonded tendons. In recent years, growing attention has been paid to the investigation, development, and application of external unbonded and internal bonded posttensioning tendon systems in segmental bridges.

Objective

This study is intended to evaluate segmental bridges with external unbonded and internal bonded posttensioning tendons and to provide recommendations for their design to achieve satisfactory performance. The selected configurations of the tested box girders were similar to those used in typical SPCBG construction. A series of tests was planned to investigate the following aspects of the performance of the SPCBGs:

1. The effect of the three-part ratio of top internal tendons to bottom internal tendons to external tendons on the structural behavior and failure modes of box girders;
2. The effect of load type on the structural behavior and failure modes of SPCBGs with external unbonded and internal bonded posttensioning tendons; and
3. An evaluation of the existing formulas for predicting the tendon stress and shear strength by comparing the results obtained from existing formulas with experiment results.

Experimental Testing Program

Test Matrix

The specimens were divided into three main groups (A–C), each containing two specimens. The test matrix is given in Table 1. Specimens in Group A (SPCBG1 and SPCBG2) were segmental box girders with internal tendons subjected to a combined load. Specimens in Group B (SPCBG3 and SPCBG4) were segmental box girders with external unbonded and internal bonded posttensioning tendons subjected to a different load. Specimens in Group C (SPCBG4 and SPCBG5) were segmental box girders with external unbonded and internal bonded posttensioning tendons subjected to bending.

Test Specimens

A schematic for the test specimens is show in Fig. 1. The SPCBGs consist of 12 segments. There were five types of segments, indicated by letters A–E. The dimensional details of a half-section of the box girder are given in Fig. 2. It was observed that the thickness of the bottom slab changed at Segment C from 12 to 10 cm and that the thickness of the web changed at Segment D from 10 to 8 cm. The specimens had a height of 60 cm from the upper surface of the top slab to the lower surface of the bottom slab, and they had a width of 150 cm at the top flange and a width of 75 cm at the bottom slab.

The male-female shear key had the same scaled dimensions as those in the actual design of the precast-concrete segment. The trapezoidal shape of the key had a base area of 10×4 cm and a top area of 8×2 cm with a depth of 1 cm.

When the segments were assembled, a very thin layer of epoxy resin, approximately 1 mm on each side, was spread on the joint surface. A prestressing force was then applied to ensure that the epoxy resin would spread uniformly.

Material Properties

The concrete compressive strength at testing was, on average, 32.2 MPa, with a corresponding SD of 3.1 MPa. The steel reinforcement was HPB235 with yield and ultimate strengths of 235 and 370 MPa, respectively. Both internal bonded tendons and unbonded external tendons contained seven wires, each of reinforcement diameter Φ5 mm. According to the data sheet provided

Table 1. Characteristics of Tested Box Girders

Specimen	Load type	Tendon type	Ratio	Applied loading mode
SPCBG1	Shear bending	Internal	2:2:0	Three-point bending
SPCBG2	Shear bending	Internal	2:4:0	Three-point bending
SPCBG3	Shear bending	External and internal	2:6:2	Three-point bending
SPCBG4	Bending	External and internal	2:6:2	Four-point bending
SPCBG5	Bending	External and internal	2:4:4	Four-point bending

Note: The ratio is a number relationship among different tendons (top internal bonded tendons:bottom internal bonded tendons:external unbonded tendons). For example, the ratio 2:6:2 means that the segmental box girder has two top internal bonded tendons, four bottom internal bonded tendons, and two external unbonded tendons.

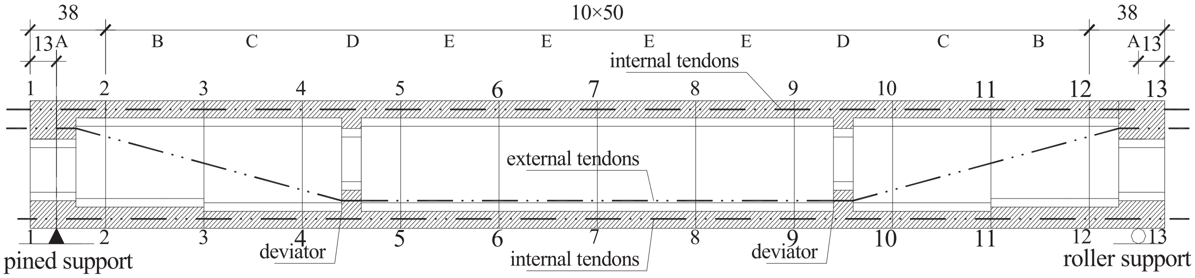

Fig. 1. Divided segment components (centimeters)

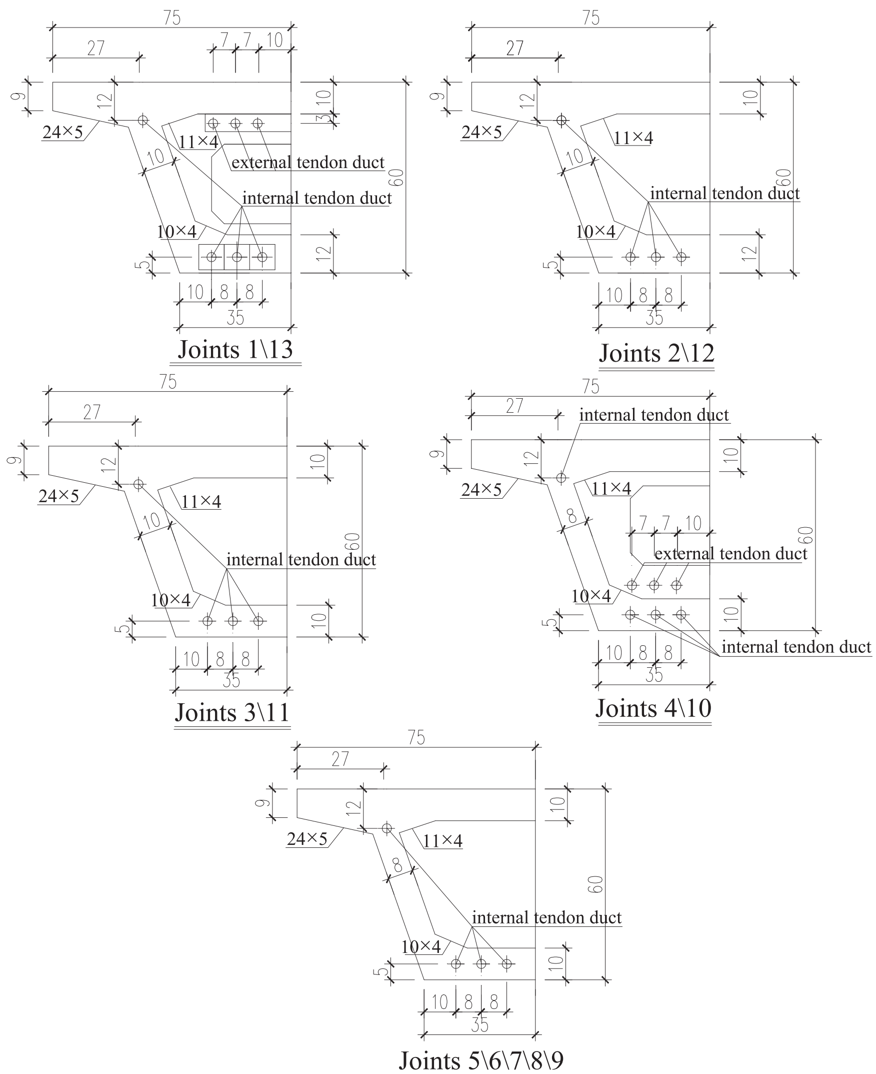

Fig. 2. Specimen dimensions and tendon allowance ducts (centimeters)

by the manufacturer, each tendon has a tensile strength of 1,860 MPa and an elastic modulus of 1.95 GPa.

Test Setup

Three of the specimens were subjected to four-point bending tests, whereas the others received a single concentrated load over the diaphragms used for deviating the tendons, as shown in Figs. 3(a and b). The vertical load was applied using a jack with a capacity of 1,000 kN; however, the prestressed load was applied using a jack with a capacity of 150 kN. All the specimens were simply supported.

The instrumentation is shown in Figs. 3(c and d). One 1,000-kN load cell was used to detect the magnitude of the applied jack load, one 300-kN load cell was used to record the magnitude of the external tendon forces and another 300-kN load cell was used to record the force variation at the anchor end, five displacement transducers (D1–D5 in Fig. 3) were used to measure the vertical displacement, and eight dial gauges were used to check joint opening along the joint.

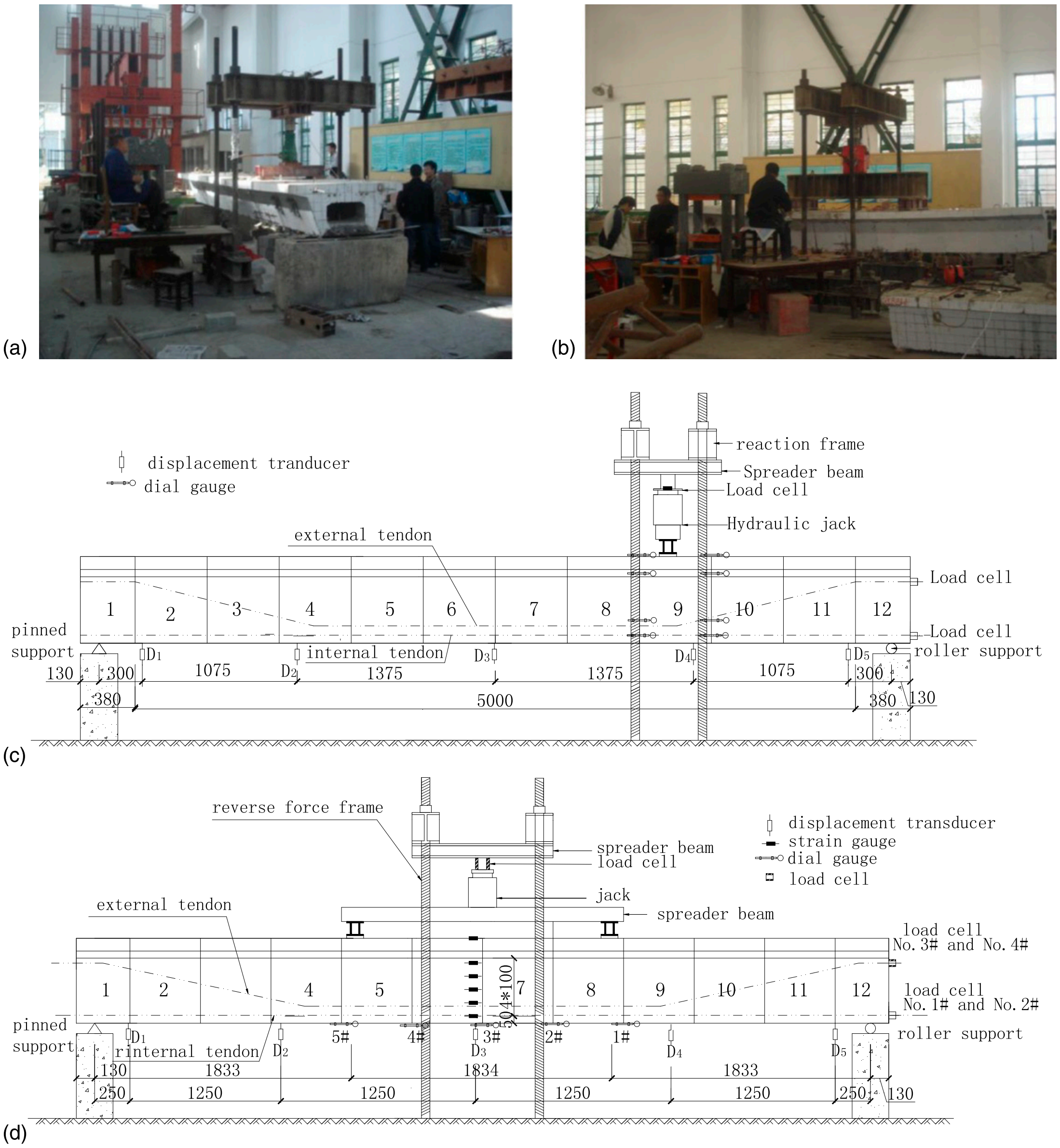

Fig. 3. Test setup and instrument layout: (a) three-point loading; (b) four-point loading; (c) instrument layout for concentrate load (millimeters); (d) instrument layout for four-point load (millimeters)

Results

Structural Response

Initially, a low prestressed load was applied to make it possible to remove the temporary supports. All the box girders were effectively prestressed before they were tested. The limitations of the control prestressing for the external and internal tendons were $0.65f_{\mathrm{ptk}}$ and $0.75f_{\mathrm{ptk}}$, respectively, where f_{ptk} is the prestressing strand-strength standard value of 1,860 MPa. This value of prestressing was determined from the load cell attached at the tendons. This means that the value of prestressing was determined after friction losses at the anchorages and deviators. The initial posttensioning forces for the external and internal tendons were 169.3 and 195.3 kN, respectively.

The vertical load was applied gradually until failure. The behavior of the box girders was evaluated in terms of vertical deformation, opening between segments, external tendon stress, load capacity, and failure mode. These behaviors will be discussed in subsequent sections.

Deformation Characteristics

Each box girder was tested under static load until complete failure. The vertical deformation of each box girder is shown in Fig. 4. As the vertical load increased, the vertical displacement of the box girder also increased gradually, and the box girder behaved as a monolithic box girder. After the load exceeded the crack moment, the joint opening and the position of the maximum deflection were near the place where the concentrated load was applied for SPCBG1, SPCBG2, and SPCBG3. However, the maximum deflection occurred at midspan for SPCBG4 and SPCBG5.

Fig. 5 shows the load–maximum vertical deflection curves for all the box girders. Initially, the load-deflection relationship was linear, but the response became slightly nonlinear until failure with further

J. Bridge Eng., 2015, 20(4): 04014075

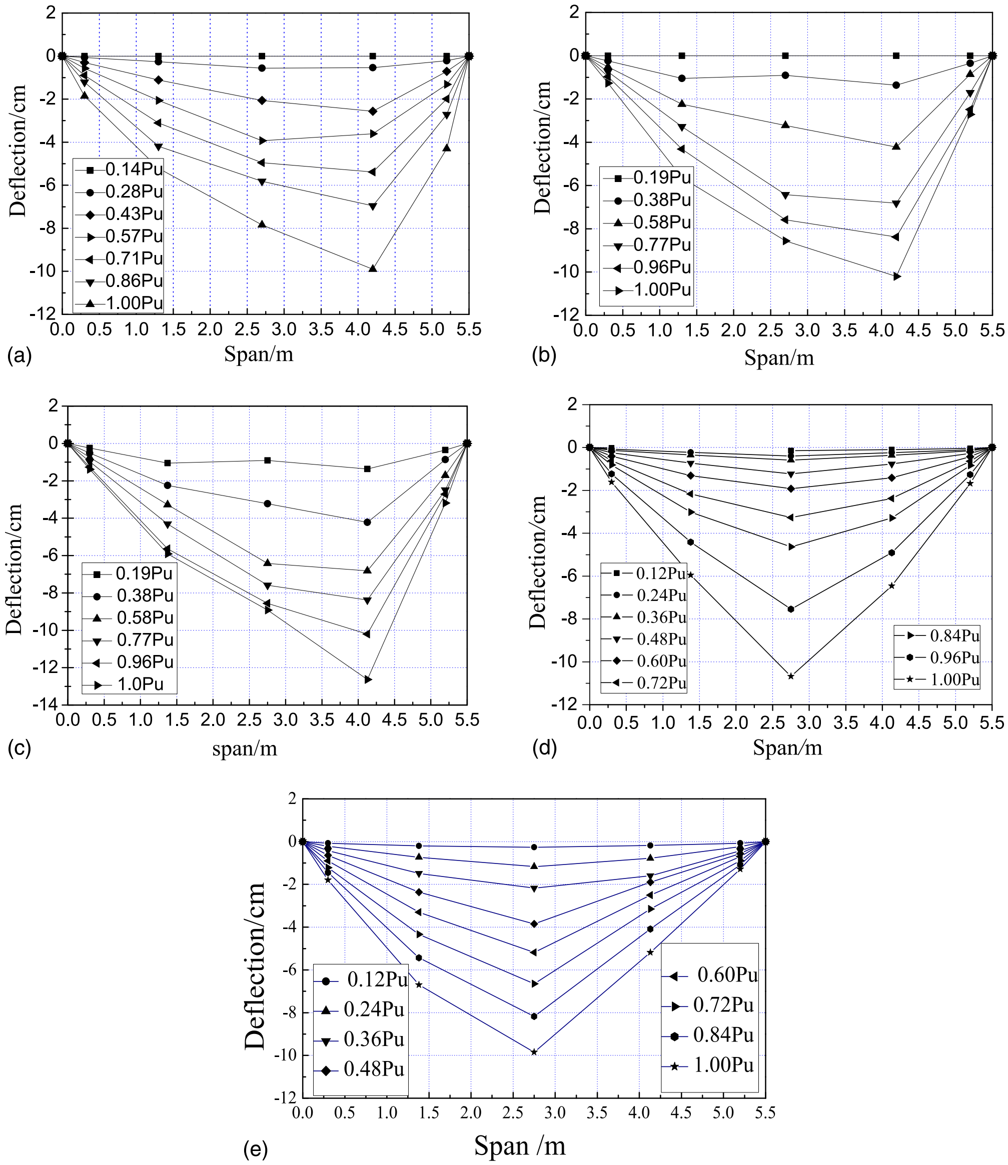

Fig. 4. Deflection along box girder under load: (a) SPCBG1; (b) SPCBG2; (c) SPCBG3; (d) SPCBG4; (e) SPCBG5

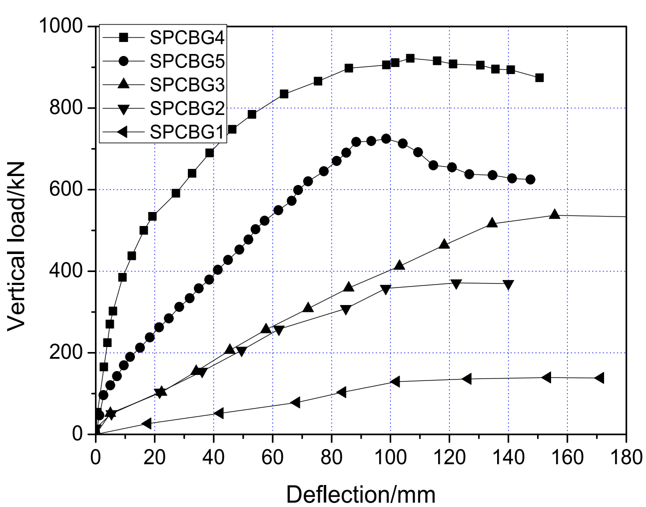

Fig. 5. Load-deflection relationship

increases of the applied load. The load-deflection relationship depends greatly on the tendon ratio and the load mode.

In the case of box girders with the same load type, the load-deflection relationships were linear up to vertical loads of 25, 45, 105, and 100 kN for SPCBG1 and SPCBG2 (Group A) and SPCBG4 and SPCBG5 (Group C), respectively. Beyond these load levels, the load-deflection relationships were nonlinear up to 139, 371, 922, and 650 kN, respectively. For SPCBG1 and SPCBG2, the more the internal bottom tendons were layouts, the higher was the load capacity achieved. For SPCBG4 and SPCBG5, although the total number of tendons was the same, the load capacity of the box girder with more internal tendons was greater than that of the box girder with fewer internal tendons.

In the case of box girders with the same tendon ratios subjected to different load types, the load-deflection relationships were linear up to vertical loads of 50 and 100 kN for SPCBG3 and SPCBG4 (Group B), respectively. Beyond these load levels, the load-deflection relationships were nonlinear up to 537 and 922 kN, respectively.

From these results, it was concluded that the tendon ratio and the load type had significant effects on the behavior of segmental box girders. All the box girders exhibited a gradual degradation in stiffness as a result of an increase in joint opening width. The nonlinear behavior resulted not only from material nonlinearity, as in a conventional RC system, but also from geometric nonlinearity resulting from opening of the interface joints between segments.

External Tendon Stress Increment

Fig. 6 shows the change in the stresses $\Delta f_{ps}/f_{pe}$ in external tendons with applied load. The rate of increase in the stresses was faster in the external tendons after joint opening than before joint opening. The difference between Box Girders SPCBG4 and SPCBG5 was that the onset point of the stress increment in SPCBG5 occurred prior to that in SPCBG4 because of the different tendon ratios. Furthermore, in a comparison of Box Girder SPCBG3 with Box Girder SPCBG4, it was concluded that the onset point of the stress increase in SPCBG3 occurred prior to that in SPCBG4 because of the different load types. SPCBG3 registered a lower stress increase onset point after opening because this box girder was subjected to three-point bending. Although the crack moments for SPCBG3 and SPCBG4 were the same because they had the same reinforcement ratios, the maximum bending moments for the girders were 1.09P for SPCBG3 and 0.93P for SPCBG4 as the applied force P increased. Obviously, SPCBG3 would reach the crack moment first under the same concentrated force. From Fig. 6, it can be concluded that the stress increases in the external tendons Δf_{ps} were approximately 30–50% of the effective prestressing stress f_{pe} at the ultimate failure load, and the different load types and different tendon ratios led to different onset points of the stress increase.

Joint Opening

The width of the joint opening was measured over a dial-gauge length (15 cm) that included one joint crack. Fig. 7 shows the width distributions along the joint measured across sections of a crack joint at the failure region with various loading increments. The position of a crack joint at the failure region with concrete crush is shown in Fig. 8. It is evident from Fig. 7 that the measured width profiles were reasonably linear. As the load increased, the compression length at the top decreased rapidly because of redistribution of stress caused by joint opening. In a comparison of Fig. 7(a) with Figs. 7(b, d, and e), it was concluded that the width of the joint opening in box girders with more internal bottom tendons was less than that for box girders with fewer internal bottom tendons. In a comparison of Fig. 7(c) with Fig. 7(d), it was also concluded that the width of the joint opening under three-point loading was larger than that for the box girder under four-point loading.

Fig. 7 also shows that the height of the compressive region for box girders with more internal bottom tendons is greater than that for box girders with fewer internal tendons and that the height of the compressive region for external unbonded and internal bonded posttensioning box girders with more internal bottom tendons is greater than that of box girders with fewer internal bottom tendons. For SPCBG1, SPCBG2, and SPCBG3, the heights of the compressive regions were approximately 3, 5, and 13 cm, respectively. For SPCBG4 and SPCBG5, the heights of the compressive regions were approximately 7 and 4 cm, respectively.

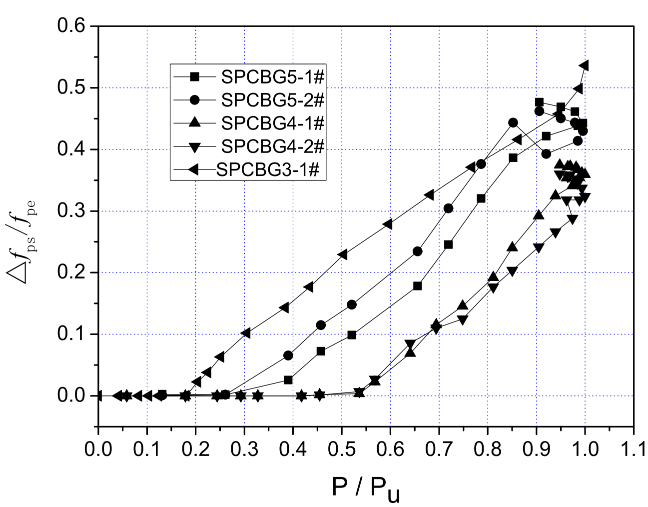

Fig. 6. Load–incremental stress relationship

Crack Pattern and Propagation

In general, as vertical loads increased, some small cracks developed near the shear keys. With a small increase in loading, the joints at maximum bending moment near the applied load open up to the top slab. Because epoxy resin was spread on the joint surface, the crack developed near the joint.

The ultimate crack pattern of each box girder is shown in Fig. 8. There is a significant difference between Fig. 8(a) and Fig. 8(b) because Box Girder SPCBG3 has external unbonded and internal bonded posttensioning tendons. The critical-failure crack was located at the joint between Segments 8 and 9 for SPCBG1 and SPCBG2, whereas it was located at the joint between Segments 9 and 10 for SPCBG3. In a comparison of Fig. 8(c) with Fig. 8(d), it was also concluded that the critical-failure crack happened in the pure bending zone and near the one-third loading point. However, for SPCBG4, the diagonal crack appeared in the web, as shown in Fig. 8(c), whereas a diagonal crack did not occur in SPCBG5. It was concluded that bend-up external tendons could improve the shear-bearing capacity of a segmental box girder.

Failure Modes

The failure modes of the simply supported segmental box girders depended mainly on their type of reinforcement and their type of load, as shown in Table 2. When failure occurred, it meant that the bearing capacity of the SPCBG decreased with the crushing of concrete at the compression zone and the yielding of internal bonded and external unbonded tendons. It was concluded that for the same tendon layouts, there was a significant difference in the failure-load capacities and failure mode for the different load types, as seen by comparing SPCBG3 with SPCBG4. On the other hand, for the same load type, a significant difference was observed in the failure-load capacities for different tendon ratios, as seen by comparing SPCBG1 with SPCBG2 and SPCBG4 with SPCBG5.

The failure modes, as shown in Fig. 9, may be summarized as follows:

- If the reinforcement ratio ρ was less than 0.1% or the SPCBG was subjected to bending, the box girder failed in flexure. The failures of SPCBG1, SPCBG4, and SPCBG5 occurred suddenly as a result of crushing of the concrete in the top flange.
- If the reinforcement ratio ρ was greater than 0.1% or the SPCBG was subjected to a concentrated load, flexural and shear failure occurred. Under the interaction of bending and shear, the failure of the tested box girders was not a pure shear failure; rather, it was produced by a combination of shear and bending. The failures of SPCBG2 and SPCBG3 occurred suddenly as a result of sliding and crushing of the concrete.

J. Bridge Eng., 2015, 20(4): 04014075

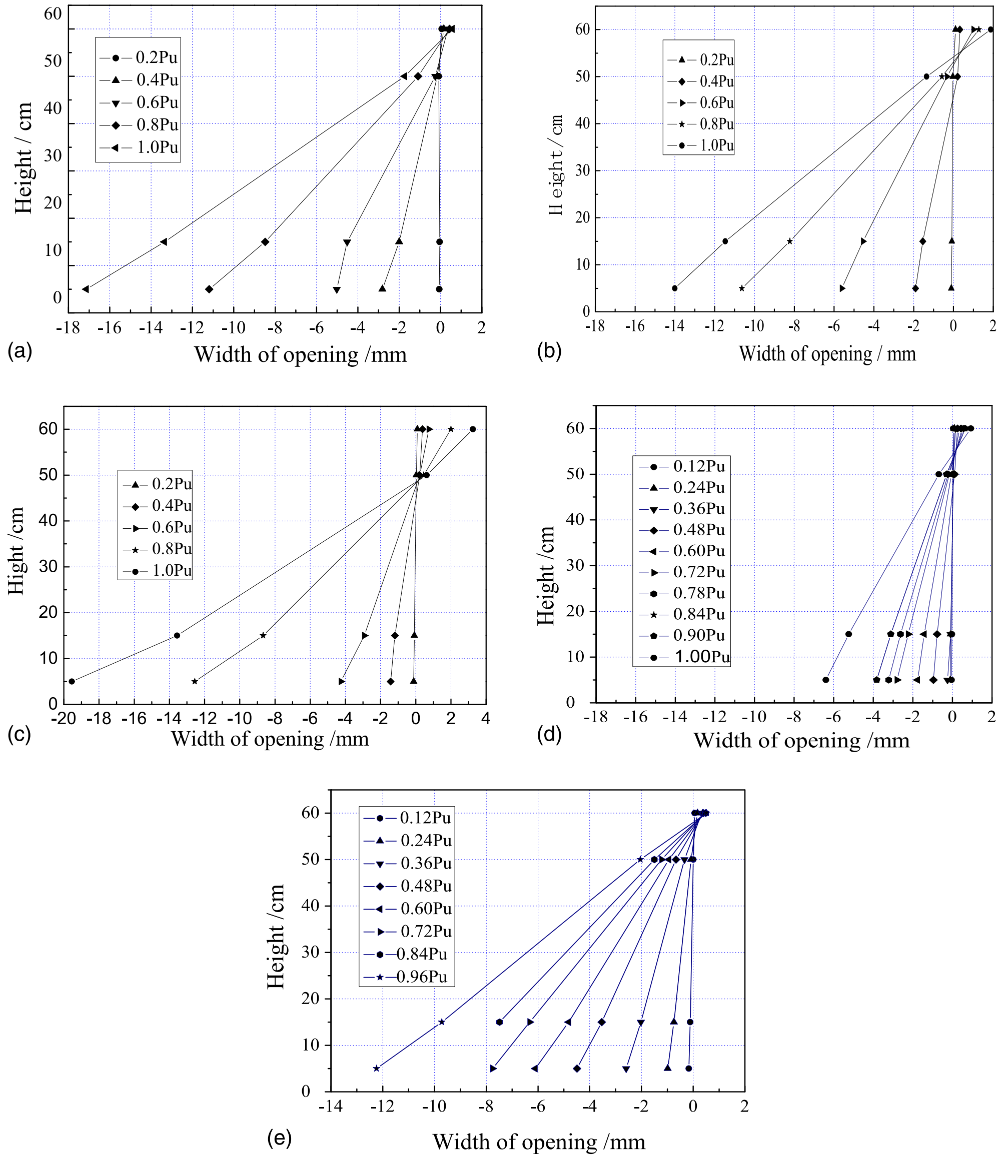

Fig. 7. Width distribution across opening joint section at various loading increments: (a) SPCBG1; (b) SPCBG2; (c) SPCBG3; (d) SPCBG4; (e) SPCBG5

Discussion

Comparison with Existing Stress Increment Calculation Formula in External Tendons

As is well known, there are two main differences between external unbonded tendons and internal bonded tendons. One is the strain incompatibility that exists between the surrounding concrete and the external unbonded tendons; the other is the second-order effect. These two features make it difficult to calculate the incremental stresses in external tendons.

Many theoretical and experimental investigations have been undertaken to study the external tendon stress increment under the ultimate limit state (Naaman and Alkhairi 1991; Harajli 2006; Dall'Asta et al. 2007). Even though much effort has been expended for several decades on the computation of the incremental stress increment of external tendon, it is still questionable whether any of the proposed methods are consistent in all situations. For the sake of brevity, only some important equations are reproduced herein.

Naaman and Alkhairi (1991) proposed the following prediction equation for the stress in external unbonded prestressing tendons (1 ksi = 1,000 psi = 6.895 MPa):

$$\Delta f_{ps} = f_{ps} - f_{pe} = \Omega_u E_{ps} \varepsilon_{cu} \left(\frac{d_p}{c} - 1 \right) \frac{L_1}{L_2} (\text{psi}) \tag{1}$$

where E_{ps} = elastic modulus of prestressing steel; L = length of span for which computation is carried out; L_1 = sum of lengths of loaded spans containing the tendon considered; L_2 = total length of the tendon between anchorages; ε_{cu} = assumed failure strain of concrete in compression (=0.0033); d_p = depth from concrete extreme compressive fiber to the centroid of prestressing steel; $\Omega_u = 3/(L/d_p)$ for uniform or third-point loading and $1.5/(L/d_p)$ for one-point midspan loading; and c = depth from concrete extreme compressive fiber to the neutral axis.

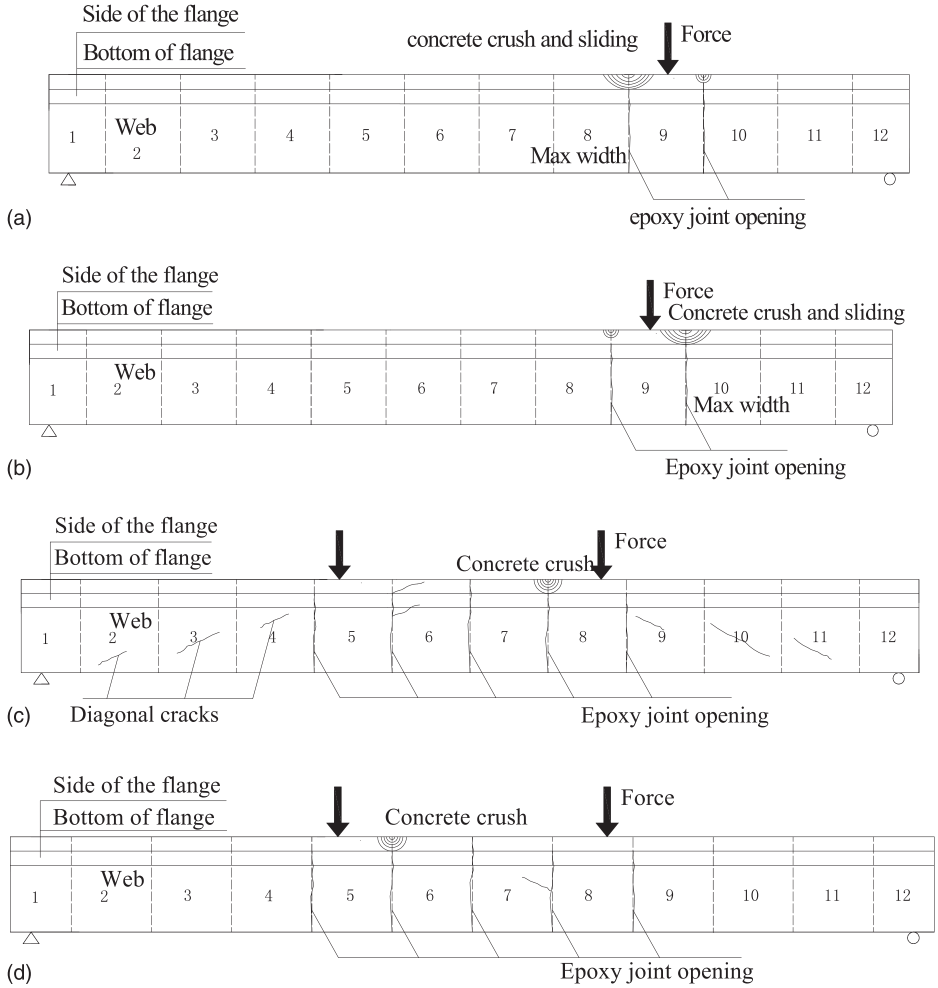

Fig. 8. Crack pattern of each box girder: (a) SPCBG1 and SPCBG2; (b) SPCBG3; (c) SPCBG4; (d) SPCBG5

Table 2. Summary of Test Results

Box-girder number	$\rho\,(A_{pe}+A_{pi})/A_c$ (%)	Failure load (kN)	Maximum deflection (cm)	Sliding distance (mm)	Failure mode
SPCBG1	0.06	139.37	15.3	No sliding	Flexural failure
SPCBG2	0.13	371.41	12.2	50	Flexural and shear failure
SPCBG3	0.26	537.18	15.6	30	Flexural and shear failure
SPCBG4	0.26	922.00	10.7	No sliding	Flexural failure
SPCBG5	0.26	724.00	10.4	No sliding	Flexural failure

AASHTO's *Guide specifications for design and construction of segmental concrete bridges* (AASHTO 1999) adopted the following equation to predict tendon stress:

$$\Delta f_{ps} = f_{ps} - f_{pe} = 6{,}300\left(\frac{d_p - c}{l_e}\right) \tag{2}$$

where

$$c = c_y = \frac{A_{ps}f_{py} + A_s f_y - A'_s f'_y - 0.85\beta_1 f'_c(b - b_w)h_f}{0.85\beta_1 f'_c b_w} \tag{3}$$

$$l_e = \left(\frac{l_i}{1 + N_s/2}\right) \tag{4}$$

f_{pe} = effective prestress after accounting for all losses; f'_c = concrete compressive strength; c_y = neutral axis depth calculated from force equilibrium across the depth of the critical section assuming that $f_{ps} = f_{py}$; l_e and l_i = effective tendon length and length of tendon between anchorages, respectively; N_s = number of support hinges required to form a mechanism crossed by the tendon; β_1 = concrete strength factor, defined in AASHTO 5.7.2.2 (AASHTO 1999); b, b_w, and h_f = flange width, web width, and flange thickness, respectively; and A_{ps}, A_s, and A'_s = area of prestressing steel, area of ordinary-tension steel, and area of compression steel, respectively.

The American Concrete Institute (ACI) code equation (ACI 2008) is written as

$$\Delta f_{ps} = f_{ps} - f_{pe} = 70 + \frac{f'_c}{\kappa\rho_p} \tag{5}$$

J. Bridge Eng., 2015, 20(4): 04014075

Fig. 9. Failure modes of each segmental box girder: (a) flexural failure of SPCBG1; (b) flexural and shear failure of SPCBG2; (c) flexural and shear failure of SPCBG3; (d) flexural failure of SPCBG4; (e) flexural failure of SPCBG5

where $\kappa = 100$ for $L/d_p \leq 35$ and $\kappa = 300$ for $L/d_p > 35$ (where L = span and d_p = depth from the extreme compression fiber to the center of the prestressing steel); and ρ_p = ratio of prestressing steel.

Harajli (1990) accounted for span-to-depth-ratio effects and proposed the following equation, which resembles Eqs. (18-4) and (18-5) in ACI 318-08 (ACI 2008):

$$\Delta f_{ps} = f_{ps} - f_{pe} = \left(10{,}000 + \frac{f_c'}{100\rho_p}\right)\left(0.4 + \frac{8}{S/d_p}\right)\text{(psi)} \quad (6)$$

where S/d_p = span depth ratios. In 2006, Harajli (2006) proposed another equation to calculate the stress increment, written as

$$\varepsilon_{ps} = \varepsilon_{pe} + \varepsilon_{cu}\left(\frac{d_p - c}{L/n}\right)\left(\frac{20.7}{f} + 10.5\right) \quad (7)$$

where $f = \infty$ for a single concentrated force and $f = 6$ for a uniform load. Using Eq. (7), three possible design alternatives can be utilized to evaluate the stress increase Δf_{ps} in unbonded internal or external tendons. These alternatives are presented and discussed in Harajli (2006). It is not necessary to list them again here.

However, many tests have shown that there is an almost linear relationship between the stress increment of external tendons Δf_{ps} and the midspan deflection δ_{mid} even near the stage of collapse. Du and Liu (2003) introduced a broken line to simplify the deformation curve of the box girder at ultimate stress. The tendon stress increment can be written as

$$\Delta f_{ps} = \frac{4E_{ps}e_m\delta_{\text{mid}}}{L^2} \quad (8)$$

where E_{ps} = modulus of elasticity of prestressing tendons; e_m = tendon eccentricity at the box-girder midspan; L = length of the span; and δ_{mid} = box-girder midspan deflection.

Based on the preceding assumption, He and Liu (2010) also proposed a practical design equation to predict the ultimate stresses of external tendons. The tendon stress increment can be given by

$$\Delta f_{ps} = \frac{\varepsilon_{cu}\delta_{\text{mid}}(\eta e_m - \phi\delta_{\text{mid}})}{L^2} \quad (9)$$

where the parameters η and ϕ depend on the load type and number of deviations, as shown in Table 3.

Based on the preceding discussion, there are many different formulas to calculate the tendon stress increment. This indicates that researchers all around the world are doing their best to develop better methods that have clear physical significance and are practical for designers.

To verify the effectiveness and accuracy of existing methods for segmental bridges with external tendons, a comparison among these formulas based on the authors' test results and other segmental girder test results is made. The accuracy of the predictions is evaluated in terms of mean value and SD. Given in these figures are the average ratio of experimental results to analytical predictions (Exp./Pre.) and corresponding SD. From Fig. 10, it can be seen that the methods of Du and Liu (2003) and He and Liu (2010) give relatively accurate results: the ratio of the mean experimental ultimate stress increment to the mean calculated ultimate stress increment is 1.05 and 1.01, with SDs of 0.98 and 1.05, respectively. The AASHTO specification (AASHTO 1999) is shown to be unconservative because the ratio of the mean experimental ultimate stress increment to the mean calculated ultimate stress increment is 0.97, but the SD of the ratio of experimental to analytical results is considerably higher (=1.72), which means that a scattering phenomenon occurs. The predictions of Harajli (1990, 2006) are reasonably conservative compared with the other equations. It also can be seen that the equation in ACI 318-08 (ACI 2008) and the expression of Naaman and Alkhairi (1991) are both overconservative in evaluating the stress increment of external tendons for segmental bridges.

Table 3. Values of η and ϕ under Some Typical Load Types and Tendon Profiles

Load case	Tendon profile	η	ϕ
One-point load	Harped with one deviation	$4-2\beta$	0.80
	Harped with two deviations	$(46-8\beta)/9$	0.45
Two-point load	Harped with one deviation	$(88-56\beta)/23$	0.94
	Harped with two deviations	$(100-24\beta)/23$	0.41

In evaluating the level of conservatism or unconservatism of the predictions of these methods, it can be seen that the equations of Du and Liu (2003) and He and Liu (2010), based on midspan deflection, are able to predict the test data more consistently and accurately,

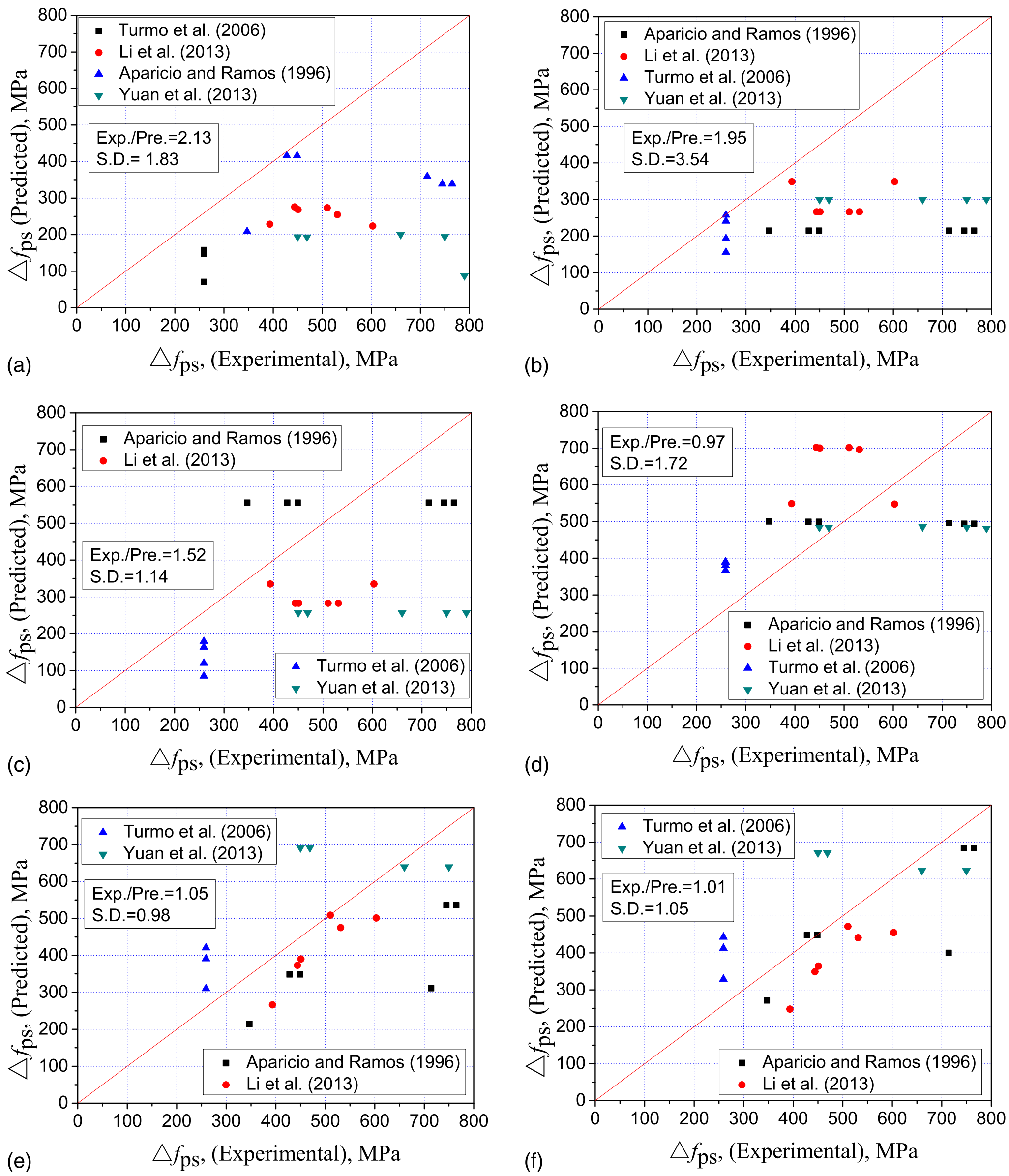

Fig. 10. Comparison of analytical Δf_{ps} predictions with experimental data: (a) Naaman and Alkhairi (1991); (b) ACI 318-08 (ACI 2008); (c) Harajli (1990, 2006); (d) AASHTO (1999); (e) Du and Liu (2003); (f) He and Liu (2010)

which is evident in the relatively low SD and better correlation between the experimental data and predicted results.

These methods, including the expression of Naaman and Alkhairi (1991), the equation from ACI 318-08 (ACI 2008), the proposed method of Haralji (1990, 2006), and the AASHTO specification (AASHTO 1999), all encounter considerable scatter in the prediction of experimental data for a segmental bridge with external tendons. One of the main reasons that these methods agree is that the effect of bonded tension reinforcement, the span-to-depth ratio, the area of bonded reinforcement, the equivalent plastic-hinge length, and the effect of loading pattern are all parameters that influence the stress in external tendons at ultimate stress. They all focus on the strain compatibility and the force-equilibrium equation at the critical section, which are key problems in bonded concrete systems. However, they may neglect the compatibility between tendon elongation between anchorages and deformation of the concrete box girder as a whole. For a segmental bridge, the failure mechanism and deformation are different from those of a monolithic bridge. For a segmental bridge with multiple dry or epoxied shear key joints, it makes no physical sense to consider that the bridge has lost its load capacity because of the tensile strain of concrete up to 0.01. When the joints open widely, the concrete and reinforcing steel are still elastic, and the deflection can be completely recovered by uploading the box girder. The tests show that actual ultimate loads depend on the compressive strain, the depth of the neutral axis, and the failure mechanism, which are much larger than those calculated using a tensile strain limit for the concrete.

Finally, it should be noted that only scarce test results for segmental box girders are available, and the recommended methods of Du and Liu (2003) and He and Liu (2010) may be incompatible with the actual loading pattern and continuous members.

Comparison with the AASHTO Standard

AASHTO (1999) specifies the formula used to estimate the shear strength of segmental beams subject to shear as

$$V_u \leq \phi V_n = \phi(V_c + V_s) \tag{10}$$

$$V_c = 0.166K\sqrt{f_c'}b_v d_v \tag{11}$$

$$V_s = \frac{A_v f_{yv} d_v}{s_v} \tag{12}$$

where V_n = nominal shear strength; V_c = nominal shear strength provided by concrete; V_s = nominal shear resisted by the stirrups; ϕ = strength reduction factor (=0.85); s_v = spacing of stirrups; b_v = effective web width; $d_v = 0.8h$ or the distance from the extreme compression fiber to the centroid of the prestressing reinforcement, whichever is greater; A_v = area of shear reinforcement within a distance s; K = stress variable computed in accordance with AASHTO 5.8.6.3 (AASHTO 1999); and f_{yv} = yield strength of reinforcing bars.

A comparison of the calculation results using Eq. (10) with the test results is plotted in Fig. 11. It can be seen that the AASHTO (1999) formula does not show good agreement with the experimental results except for SPCBG2. Therefore, the AASHTO formula is not suitable for calculating the shear resistances of SPCBGs. This may be attributed to the failure modes of SPCBGs. Under monotonic vertical loading, the failure cracks caused by the bending moment began in the downward surface of the bottom slab adjacent to the joint, not exactly in the interface of the two segments. Then the joint continued opening, and the cracks started to propagate to the top flange as the loads applied to the models were increased. Finally, the failure occurred in the plane of concrete adjacent to the epoxied joint with the crushing of the concrete in the top flange. Such failure modes mean that no diagonal cracks from the support to the loading point appeared and that stirrups contribute nearly nothing to the joint bearing capacity. However, in the AASHTO formula, the shear resisted by the stirrups is considered, but the vertical components of the prestressing tendons and the friction between the flat surfaces of two adjacent segments are ignored. Therefore, the shear formula proposed by AASHTO (1999) should be improved.

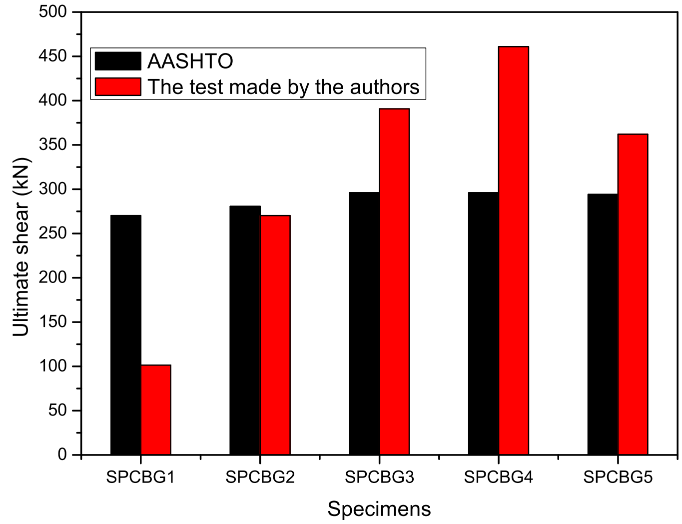

Fig. 11. Comparison of calculated and experimental results

Conclusion

An experimental study on the behavior of segmental prestressed-concrete box girders is presented in this paper. Five large-scale specimens were tested. A comprehensive assessment of several equations to predict the stress increase in external tendons and the shear strength of segmental bridges are discussed. Some important conclusions are as follows:

1. Different load types lead to different deformations (Fig. 4). A three-point bending load reduced the vertical load and vertical deflection at the onset point of nonlinearity. The openings between the segments and crushing of the concrete compression region were the main reasons for the nonlinear behavior of SPCBGs. For all the box girders, a gradual degradation in stiffness as a result of increasing deflection was observed.
2. The stress increases in the external tendons Δf_{ps} were approximately 30–50% of the effective prestressing stress f_{pe} at the ultimate failure load, and the different load types and tendon ratios led to different onset points for the stress increase.
3. The width distribution along the joint with various loading increments was reasonably linear. The width of the joint opening was influenced by the tendon ratios and load types (Fig. 7). The cracks in epoxied joints developed in the concrete adjacent to the segment interface, which was different from those in dry joints, which occurred in the segment interface.
4. The critical-failure crack was located at the joint near the applied load. The increased use of bend-up external tendons improved the shear bearing capacity of segmental box girders and avoided the appearance of diagonal cracks in the web.
5. The tendon ratio had a significant effect on the failure behavior of SPCBGs. The more internal bonded tendons that were used, the higher was the load capacity achieved. If the reinforcement

ratio ρ was less than 0.1% or the segmental box girder was subjected to bending, flexural failure occurred. If the reinforcement ratio ρ was greater than 0.1% or the segmental box girder was subjected to a concentrated load, flexural and shear failure occurred. The latter failure mode was attributed to segment sliding and to crushing of the concrete in the top slab. The failure of the shear-tested box girders was the result of a combination of shear and bending.

6. Most of the proposed design equations for evaluating the stress increase in unbonded external tendons at ultimate stress are conservative and encounter scatter in predicting experimental data because they neglect the compatibility between tendon elongation between anchorages and deformation of the concrete box girder as a whole. Eqs. (8) and (9) were recommended for the calculation of ultimate stress in the external tendons of segmental bridges.
7. The strength reduction factor used in AASHTO (1999) to reflect joint influences is not enough. Different failure modes mean different shear transfer mechanisms, and the effect of the stirrups, the prestressing tendons, and the friction between two segments should be considered.

Acknowledgments

This study was funded by the Doctoral Fund of the Ministry of Education of China (Grant No. 20100094120013), the Transportation Science Project of Jiangsu Province (Grant No. 2013Y11), and the Natural Science Foundation of Jiangsu Province (General Program, Grant No. BK2011748). The financial support of these organizations is gratefully acknowledged.

References

AASHTO. (1999). *Guide specifications for design and construction of segmental concrete bridges*, 2nd Ed., Washington, DC.

Algorafi, M. A., Ali, A. A. A., Othman, I., Jaafar, M. S., and Anwar, M. P. (2010). "Experimental study of externally prestressed segmental beam under torsion." *Eng. Struct.*, 32(11), 3528–3538.

American Concrete Institute (ACI). (2008). "Building code requirements for structural concrete and commentary." *ACI 318-08*, Detroit.

Aparicio, A. C., and Ramos, G. (1996). "Flexural strength of externally prestressed concrete bridges." *ACI Struct. J.*, 93(5), 512–523.

Aparicio, A. C., Ramos, G., and Casas, J. R. (2002). "Testing of externally prestressed concrete beams." *Eng. Struct.*, 24(1), 73–84.

Below, K. D., Hall, A. S., and Rangan, B. V. (1975). "Theory for concrete beams in torsion and bending." *J. Struct. Div.*, 101(8), 1645–1660.

Bennett, R. M., Hufstetler, M. L., and Carver, M. (2002). "50-year-old prestressed segmental concrete bridges." *J. Prof. Issues Eng. Educ. Pract.*, 10.1061/(ASCE)1052-3928(2002)128:2(83), 83–87.

Dall'Asta, A., Ragni, L., and Zona, A. (2007). "Simplified method for failure analysis of concrete beams prestressed with external tendons." *J. Struct. Eng.*, 10.1061/(ASCE)0733-9445(2007)133:1(121), 121–131.

Du, J. S., and Liu, X. L. (2003). "Research on the variations of unbonded prestressed tendon stresses based upon the structural deformation." *China Civil Eng. J.*, 36(8), 12–19.

Harajli, M. H. (1990). "Effect of span-depth ratio on the ultimate steel stress in unbonded prestressed concrete members." *ACI Struct. J.*, 87(3), 305–312.

Harajli, M. H. (2006). "On the stress in unbonded tendons at ultimate: Critical assessment and proposed changes." *ACI Struct. J.*, 103(6), 803–812.

He, Z.-Q., and Liu, Z. (2010). "Stresses in external and internal unbonded tendons: Unified methodology and design equations." *J. Struct. Eng.*, 10.1061/(ASCE)ST.1943-541X.0000202, 1055–1065.

Li, G., Yang, D., and Lei, Y. (2013). "Combined shear and bending behavior of joints in precast concrete segmental beams with external tendons." *J. Bridge Eng.*, 10.1061/(ASCE)BE.1943-5592.0000453, 1042–1052.

Megally, S., Veletzos, M. J., Bunnell, K., Restrepo, J. I., and Seible, F. (2009). "Seismic performance of precast concrete segmental bridges: Summary of experimental research on segment-to-segment joints." *J. Prestressed Concr. Inst.*, 54(2), 116–142.

Misic, J., and Warwaruk, J. (1975). "Strength of prestressed solid and hollow beams subjected simultaneously to torsion, shear, and bending." *ACI J.*, 55, 515–545.

Muller, J. (1980). "Construction of the Long Key Bridge." *J. Prestressed Concr. Inst.*, 25(6), 97–111.

Naaman, A., and Alkhairi, M. (1991). "Stress at ultimate in unbonded post-tensioning tendons. Part 1: Evaluation of the state of the art." *ACI Struct. J.*, 88(5), 641–651.

Ramos, G., and Aparicio, A. C. (1996). "Ultimate analysis of monolithic and segmental externally prestressed concrete bridges." *J. Bridge Eng.*, 10.1061/(ASCE)1084-0702(1996)1:1(10), 10–18.

Rabbat, B. G., and Sowlat, K. (1987). "Testing of segmental concrete girders with external tendons." *J. Prestressed Concr. Inst.*, 32(2), 86–107.

Rabbat, B. G., and Sowlat, K. (1990). "Behavior of 1:5-scale segmental concrete girders with external and internal tendons." *Special Publication 120-14*, American Concrete Institute, Detroit, 305–314.

Rombach, G. A. (2002). "Precast segmental box girder bridges with external prestressing: Design and construction." *Segmental Bridges*, 19(2), 1–15.

Turmo, J., Ramos, G., and Aparicio, A. C. (2005). "FEM study on the structural behaviour of segmental concrete bridges with unbonded prestressing and dry joints: Simply supported bridges." *Eng. Struct.*, 27(11), 1652–1661.

Turmo, J., Ramos, G., and Aparicio, A. C. (2006). "Shear behavior of unbonded post-tensioned segmental beams with dry joint." *ACI Struct. J.*, 103(3), 409–417.

Wouters, J. P., Kensner, K., and Poston, R. W. (1999). "Tendon corrosion in precast segmental bridges." *Transportation Research Record 1211*, Transportation Research Board, Washington, DC, 128–132.

Yuan, A., Dai, H., Sun, D., and Cai, J. (2013). "Behaviors of segmental concrete box beams with internal tendons and external tendons under bending." *Eng. Struct.*, 48(Mar), 623–634.